We are IntechOpen, the world's leading publisher of Open Access books Built by scientists, for scientists

4,800
Open access books available

122,000
International authors and editors

135M
Downloads

Our authors are among the

154
Countries delivered to

TOP 1%
most cited scientists

12.2%
Contributors from top 500 universities

WEB OF SCIENCE™

Selection of our books indexed in the Book Citation Index in Web of Science™ Core Collection (BKCI)

Interested in publishing with us?
Contact book.department@intechopen.com

Numbers displayed above are based on latest data collected.
For more information visit www.intechopen.com

4

Energy Transfer in Ion– and Laser–Solid Interactions

Alejandro Crespo-Sosa
Instituto de Física, Universidad Nacional Autonoma de México
México

1. Introduction

While the fundamentals of ion beam interaction with solids had been studied as early as the 1930s, its utility in the modification of materials was not fully recognized until the 60's and 70's. About the same time, the fabrication of high–power lasers permitted their application in the processing of materials, especially the use of short-pulsed lasers. Both techniques are nowadays widely used in a great variety of applications. The electromagnetic radiation (or photons, from a quantum mechanical point of view) from lasers interact with the electrons of the materials, transferring energy to them within femtoseconds. Energetic ions also transfer part of their energy to the electrons of the solid, but they can also interact directly with the nuclei in elastic collisions. The primary energy transferred involved in these precesses is not thermal and some assumptions must be made before treating the problem as a thermal one. Furthermore, these processes take place in very short periods of time and are localized in the nanometer range. This means that the system can hardly satisfy the condition of thermodynamic equilibrium. Despite the complexity of these processes, many of the effects on the materials can be understood by using simple classical concepts contained in the heat equation.

During the last decades, different aspects of the ion–solid interaction have been incorporated in the calculation of the temperature evolution in the so–called thermal spike. This implementation has been possible in part, by the development of fast computers, but also by the availability of ultra short laser pulses that have given a great amount of information about the dynamics of electronic processes Elsayed-Ali et al. (1987); Schoenlein et al. (1987); Sun et al. (1994)). From a thermal point of view, these processes are very similar either for ions or for lasers pulses. The results obtained in one case can be applied most of the times to the other. For many of these experimental phenomena, the estimation of the temperature is only the first step and supplementary diffusion or stress equations must be solved, consistent with the spatial temperature evolution in order to describe them.

From another point of view, nano–structures are nowadays of great interest in technology. Nano–structured materials have opened the possibility to fabricate smaller, more efficient and faster devices. Thus, the fabrication and characterization of new nano–structured materials has become very important and the use of ion beams and short laser pulses have proved to be quite appropriate tools for that purpose (Klaumunzer (2006); Meldrum et al. (2001); Takeda & Kishimoto (2003)). Thus, their modeling and understanding is very important.

It is shown, in this chapter, firstly, how the the "thermal spike" model has recently incorporated detailed aspects of the ion–solid interaction, as well as from the dynamics of the electronic system up to a high grade of sophistication. Then some experimental effects of ion beams on nano–structured materials are presented and discussed from a point of view of the thermal evolution of the system. Finally some examples of the effects of short laser pulses on nano–structured materials are also discussed.

2. The thermal spike

The concept of thermal spike in ion–solid interaction, is the result of assuming that the ion deposits an amount of energy F_D, increasing the local temperature and that thereafter it obeys the classical laws of heat diffusion. The temperature is therefore, a function of time and location and can be calculated with the aid of the heat equation:

$$\frac{\partial T}{\partial t} = \frac{1}{\rho c_p} \nabla \left[\kappa \nabla T \right] + \frac{1}{\rho c_p} s(t, \vec{r})) \tag{1}$$

where T is the temperature as function of time t and position $\vec{r}$, and $s(t, \vec{r})$ is, in general, a source or a sink of heat, that can also be a function of time t and position $\vec{r}$. In the simplest model, the source $s(\vec{r}, t)$ is taken as a Dirac delta function in time and space. If it is assumed that the energy is deposited at a point, spherical thermal spike comes to one's mind, while if it is deposited along a straight line, the spike is said to be cylindrical. Vineyard (Vineyard (1976)) solved this equation and further calculated the total number of atomic jumps produced by the ion within the spike using the temperature evolution within it and an jumping rate proportional to $\exp(-\frac{E}{k_B T})$. Because of its simplicity, this model is still widely used to estimate the "temperature" of the thermal spike, whether it is an elastic spike due to nuclear stopping power or the so-called inelastalic spike due to electronic interaction.
In the two-temperature model, the energy transfer from the electrons to the lattice is considered with a second equation coupled with the first through an interaction term $g(t, \vec{r})$:

$$\frac{\partial T_e}{\partial t} = \frac{1}{\rho c_{p_e}} \nabla \left[\kappa_e \nabla T_e \right] + \frac{1}{\rho c_{p_e}} s_e(t, \vec{r})) - \frac{1}{\rho c_{p_e}} g(t, \vec{r}) \tag{2}$$

$$\frac{\partial T_l}{\partial t} = \frac{1}{\rho c_{p_l}} \nabla \left[\kappa_l \nabla T_l \right] + \frac{1}{\rho c_{p_l}} s_l(t, \vec{r})) + \frac{1}{\rho c_{p_l}} g(t, \vec{r}) \tag{3}$$

here, the subscript e stands for electron, while l for lattice, and $g(t, \vec{r})$ is the electron–phonon coupling term that allows the heat transfer from the electronic subsystem to the lattice via electron–phonon scattering (Lin & Zhigilei (2007); Toulemonde (2000); Wang et al. (1994)). Free electrons contribute at most to electronic conductivity, so that it is larger for metals than for semiconductors or dielectrics.
At higher ion energies, that is when the electronic interaction prevails, the geometry of the spike is that of the global spike along the whole ion's path, however the energy deposition cannot be considered instantaneous nor one-dimensional (Waligórski et al. (1986))Katz & Varma (1991). The energy of the ejected electrons is high and therefore their range (tens of nanometers) is needed to be taken into account. For an ion with velocity v, the radial energy distribution density is given by:

$$D(r) = \frac{Ne^4 Z^{*2}}{am_e c^2 \beta^2} \left[\frac{\left(1 - \frac{r+R}{T+R}\right)^{1/a}}{(w+I)^2} \right] \tag{4}$$

where R is the range of an electron with energy I and T is the maximum range, corresponding to the maximum possible energy transfer. Finally, the temporal component can be included (Toulemonde (2000); Toulemonde et al. (2003; 1992); Wang et al. (1994)) and then, the source of heat $s_e(r,t)$ in Eq. 2 is:

$$s_e(r,t) = s_0 D(r) \exp\left(-\frac{(t-t_0)^2}{2{t_0}^2}\right) \tag{5}$$

here, t_0 is the mean flight time of the electrons and the width of the gaussian function has also been set to t_0 ($\approx 10^{-15}$ s).
The main effect of the energy deposition and subsequent temperature rise is the formation of tracks in dielectrics and some metal alloys (Toulemonde et al. (2004)). As the ion moves along the material, the heat provokes melting of the matrix with a corresponding expansion and structure change. Even though the material cools down again, the quenching rate is too fast for a full reconstruction and an amorphous volume is left, if the original structure was crystalline, or else, with an important amount of defects.
The description of the formation of tracks in insulators has been successfully described by means of Eq. 2 and considering the energy input given by Eq. 5. With this model, it is possible to explain quantitatively the dimensions of the latent tracks left in insulators, as well as sputtering observed in this regime (Toulemonde (2000); Toulemonde et al. (2003)). It has been compared, in a rather complete calculation (Awazu et al. (2008)), that because gold's electronic heat conduction is very high, no melting occurs and no track is left when irradiated with 110 MeV Br ions, contrary to the case of SiO_2, where tracks are formed. This, is in agreement with experimental observations.
The implementation of the two-temperature model in metals is straightforward, as far as the electronic subsystem is composed mostly by free electrons, for which kinetic theory can give good estimates of the thermal properties. The model, as mentioned above, has also been adapted and widely used to semi–conductor and insulator materials (Chettah et al. (2009)), Recently, the model has been treated with further detail for semi-conductors (Daraszewicz & Duffy (2010)) by incorporating the fact, that the total number of conduction electrons equals the number of holes:

$$\frac{\partial N}{\partial t} + \nabla J = G_e - R_e \tag{6}$$

Here, N is the concentration of electron–hole pairs, J is the carrier current density and G_e an R_e are the source and sink of conduction electrons. The carrier current density is related with the electronic temperature by:

$$J = -D\left(\nabla N + \frac{2N}{2k_B T}\nabla E_g + \frac{N}{2T_e}\nabla T_e\right) \tag{7}$$

where D is the ambipolar diffusivity and E_g is the value of the band gap. While the validity of the additional hypothesis is beyond any doubt, its solution becomes very complicated and additional simplifications must also be added. The magnitude of the resulting correction is still to be investigated.

Another approach has been proposed by Duffy and co-workers (Duffy et al. (2008); Duffy & Rutherford (2007)). They have coupled a molecular dynamics simulation for the lattice subsystem, while the electronic one is described by Eq. 2. In this equation, $s_e(t,\vec{r})$ is then the term corresponding to the electronic stopping power and $g(t,\vec{r})$ is the usual electron–phonon coupling term between the two subsystems. This approach permits a direct quantification or the radiation damage and has allowed to show, with an Fe target, that the material can be above the melting temperature without actually melting.

3. Ion beam effects on nano–structured materials

It is known, that ion irradiation causes dielectrics and some metal alloys to expand in a direction transversal to the ion's path as a consequence of the track formation (Ryazanov et al. (1995); Toulemonde et al. (2004); Trinkaus (1998); van Dillen et al. (2005)). This effect is particularly noticeable in dielectric nano–particles and is very important as it offers an effective method to tailor the shape of dielectric nano–particles by controlling the ion's energy, fluence and irradiation angle. The modeling of this effect has been performed at the nanoscale by solving the equation of mechanical stress that results from the increase of temperature inside the ion's track (Klaumunzer (2006); Schmidt et al. (2009); van Dillen et al. (2005)). As these equation are complex by themselves, a uniform, effective track temperature is considered to solve them, nevertheless it is possible to quantitatively reproduce the experimentally measured deformation rates.

On the contrary, when metallic nano-particles embedded in SiO_2 are irradiated with high energy ions, they are deformed in the direction of the ion's path (D'Orléans et al. (2003); Oliver et al. (2006); Penninkhof et al. (2003); Ridgway et al. (2011)).

The deformation of metallo–dielectric core–shell colloids under MeV ion irradiation was extensively studied by Penninkhof and co-workers (Penninkhof et al. (2003; 2006)). They found, that while the dielectric shell deformed perpendicularly to the ion beam, the metallic core was elongated along the ion's path. They proposed a kind of passive deformation mechanism, in which the metallic core was a consequence of the well-known deformation of the dielectric material. However, when they studied the deformation of Ag, and Au nano–particles embedded in thin soda–lime films, they observed no deformation of the Ag nano–particles, suggesting that thermodynamic parameters of the metal were also involved in the deformation mechanism.

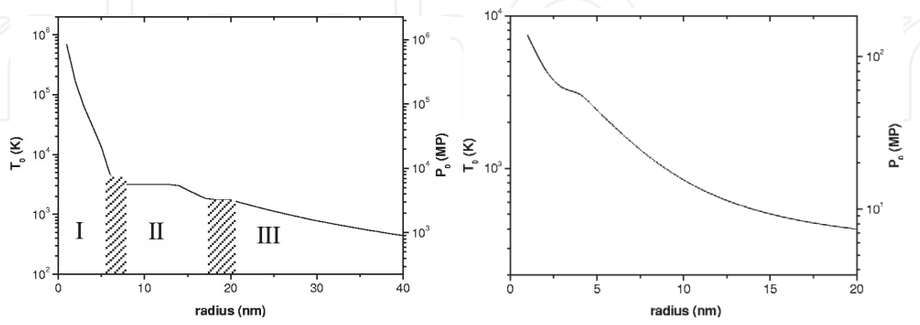

(a) Nano–particles temperature (b) Spike temperature

Fig. 1. (a) Temperature reached by the nano–particle as function of its radius, after the ion has passed through it. (b) Temperature of the substrate at a distance r from the ion's path after 10^{-12} s according to D'Orléans et al. (2003).

D'Orleans et. al. (D'Orléans et al. (2003; 2004); D'Orléans, et al. (2004)) have studied thoroughly the elongation of Co nano–particles by 200 MeV Iodine ions. They proposed a simple model, in which the ion goes through the nano–particle. As the stopping power is larger in the metal than in the matrix, and as metal conductivity is also larger, they considered that the energy deposited at the nano–particle with radius r is transformed entirely within it into heat to raise its temperature. So, they found that very small nano–particles reach evaporation temperature, while very large do not melt. The intermediate sized nano–particles that reach up to liquid temperature are subjected to thermal stress. Fig. 1 shows their calculation in which they determine, that after 10^{-12} s the temperature at the center of the track is higher than the nano–particles temperature, but that the thermal stress (right axis), $\Delta P = \frac{\alpha}{\chi}\Delta T$, is lower due to differences in the expansion coefficient α and the compressibility χ with the metal. The time 10^{-12} s is taken for the comparison, as it is the typical time for reaching equilibrium between the electronic and lattice systems. Simple though this model might seem, it has the virtue of putting emphasis firstly on the active role that nano–particles play (it is not a consequence of the transversal expansion of the matrix), and secondly on the importance of thermal stress and thermal parameters diferences of the materials involved.

Awazu has performed calculations for 110 MeV Br, 100 MeV Cu and 90 MeV Cl ions impinging on Au rods embedded in SiO_2 based on the two-temperature model (Eq. 2), and has shown some details of the thermal conduction process (Awazu et al. (2008)). Even though the electronic conductivity of the metal is very high, the border of the nano–particle limits the conduction, allowing the temperature to raise above the melting point, a requirement that has been established to be necessary for the deformation to take place.

Silver and gold nano–particles, embedded in silica, irradiated with 8–10 MeV Si ions exhibit a similar behavior (Oliver et al. (2006); Rodríguez-Iglesias et al. (2010); Silva-Pereyra et al. (2010)), This case, is similar to the previous one, but in a smaller scale. The energy deposited by the ion is lower, and so are the nano–particles that can be elongated, as well as the track radius, as shown in Fig. 2. The difference in thermal stress remains and therefore the same explanation is applicable. It had been observed before that silver ions migrate and evaporate out of the matrix when the samples are annealed at temperatures close to 1000 °C (Cheang-Wong et al. (2000)), therefore, it is suggested that not only does the thermal stress plays an important role, but also the increase of the metal solubility in the matrix, allowing ions to move preferentially through the track and aggregating again at the cooling stage of the thermal spike.

Because of the high electrical conductivity of silver and gold, the surface plasmon resonance is very well defined, so that the shape of the nano–particles can be characterized optically by it and by its splitting when they are ellipsoid instead of spheres. Fig. 3 (a) shows this effect as function of the geometry. When the wave vector is parallel to the major axis and the electric field is therefore perpendicular, only the minor axis mode can be excited and only one resonance observed. Otherwise, two resonances are observed, with relative intensities depending on the angle of orientation. In Fig. 3 (b) the selection of the excitation mode is obtained by changing the light polarization to excite either the minor or the major axis. If we know the geometry used for the irradiation, we can determine that there are two minor axes and one major axis.

Electron microscopy has given additional evidence of the deformation and detailed information on the microstructure of the nano–particles, as shown in Fig. 4. Furthermore, it has also allowed the in-situ observation of the effect that the electron beam has on the

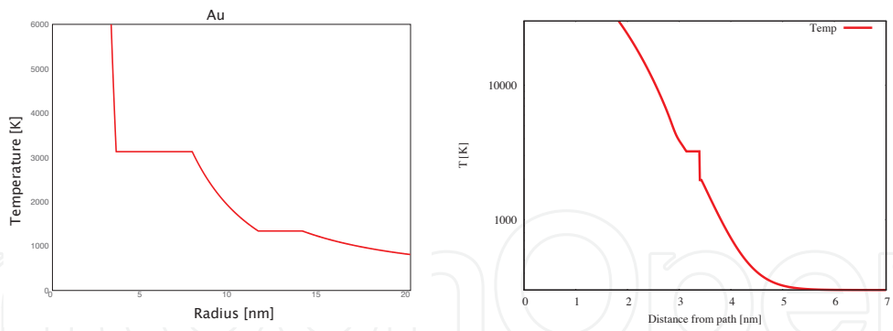

(a) Nano–particles temperature (b) Spike temperature

Fig. 2. (a) Temperature reached by gold nano–particles as function of its radius, after the ion has passed through it. (b) Temperature of the SiO_2 substrate at a distance r from the ion's path after 10^{-12} s.

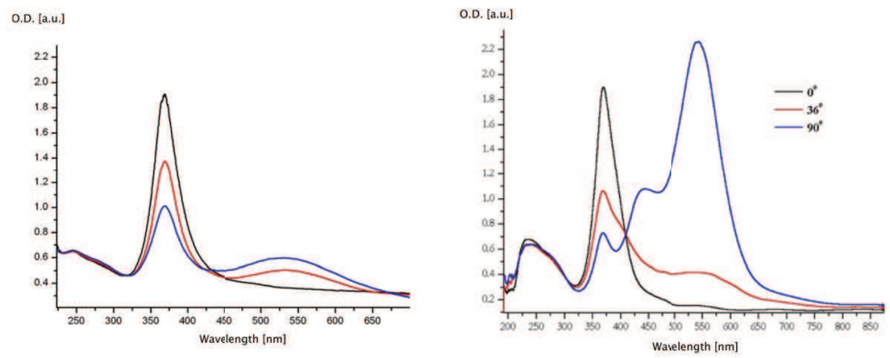

(a) Surface plasmon resonances, as function to the orientation angle.

(b) Surface plasmon resonances, as function to the polarization angle.

Fig. 3. Optical analysis of metallic nano–particles embedded inside SiO_2. When they are prolate ellipsoids, two resonant modes appear instead of one

elongated nano–particle: they recover their spherical shape without melting (Silva-Pereyra (2011); Silva-Pereyra et al. (2010)).

Ridgway and co-workers (Giulian et al. (2008); Kluth et al. (2009; 2007); Ridgway et al. (2011)) have shown that this effect is also present when Pt, Cu and Au nano–particles are irradiated with Sn and Au ions at different energies above 100 MeV. They have shown many new features of the phenomena, from which two attract attention. Firstly, that when nano–particles elongate, the minor axis reaches a limiting value, less than, but in correspondence with the track radius formed by the ion. And secondly, that nuclear interaction can also activate the elongation or can cause structure transitions in the nano–particles. They have even provided significant evidence of an amorphous Cu phase (Johannessen et al. (2008)).

Sapphire is a harder material and it has an expansion coefficient higher than SiO_2. For this reason, thermal stress is higher and becomes comparable to that of the metallic nano–particles. We have begun studying the induced anisotropic deformation caused by 6–10 MeV Si ions. Samples were prepared using the same methodology as above (Mota-Santiago et al. (2011; 2012)). Our preliminary results show that nano–particles do expand along the ion's path.

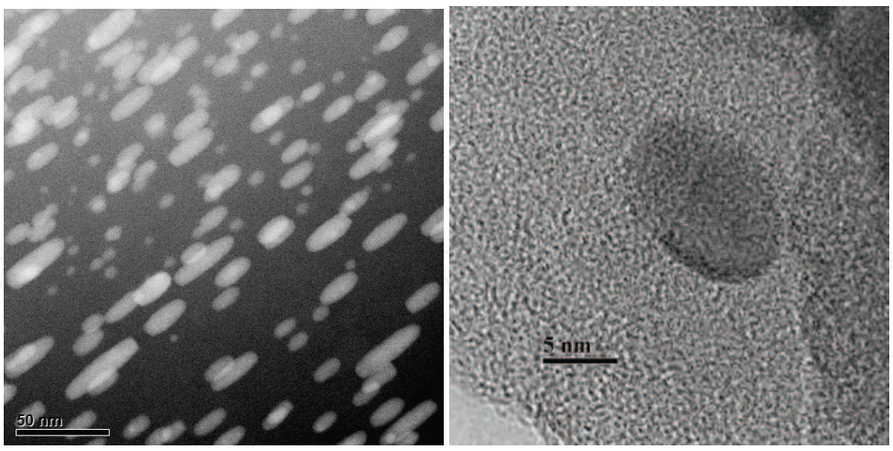

(a) Panoramic veiw (b) Single nano–particle

Fig. 4. Electron microscopy images showing the elongation of gold nano–particles by Si ions. (Rangel-Rojo et al. (2010))

Nevertheless, as the refractive index is higher (1.76), the separation of the two plasmon resonancess is not complete (Fig. 5) and the preparation of samples for microscopy is still in course of obtaining the appropriate images.

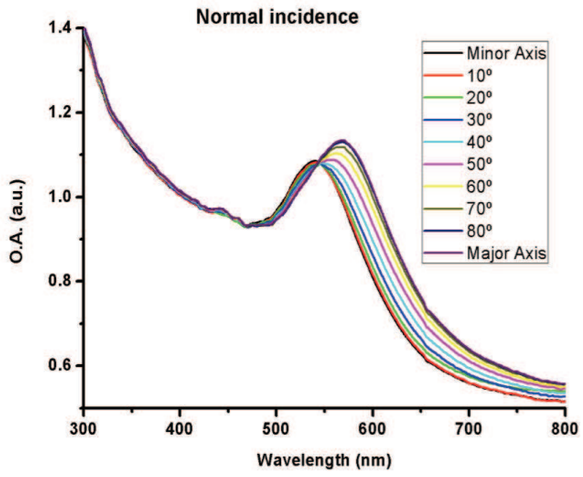

Fig. 5. Extinction spectra of Gold nano–particles in sapphire taken at different polarization angles.

Apart from being a very interesting problem from the fundamental point of view, it is worth mentioning that the control of the shape of the nano–particles by means of ion irradiation is of interest for their potential technological applications. Ag and Au nano–particles could be used in photo–electronic devices, while Co nano–particles could have magnetic applications. This reason is an additional motivation to further study the mechanisms of the deformation. Currently, many groups are working experimentally as well as theoretically to better describe the effect.

4. Laser effects on nano–structured materials

The fact that ballistic effects are minimal in laser–solid interactions, simplifies greatly the theoretical description of laser–solid interaction and its effects, while the probability to control the duration of the pulse allows the experimental determination of the characteristics of the process. If the irradiance of the laser pulse is given by $I = I_0 \exp((t - t_0)^2/2\sigma^2)$, the energy absorbed at $\vec{r}$ is simply

$$s(\vec{r}, t) = \alpha(\vec{r}) I(\vec{r}) \exp((t - t_0)^2/2\sigma^2) \tag{8}$$

where α is the absorption coefficient of the material. A deeper description of these phenomena is to be found elsewhere in this book (Sands (2011)). An important parameter to be considered when describing laser effects, is the heat diffusion length l, that tells us how long heat has travelled after time t. It is defined as:

$$l = \sqrt{\frac{\kappa t}{\rho c_p}} \tag{9}$$

For example, when this length for the duration of the laser pulse is longer than the radius of the nano–particle, the calculation can be done by considering the system as homogeneous, as shown previously in (Crespo-Sosa et al. (2007)), where the thermal effects of excimer laser pulses on metallic nano–particles embedded in a transparent matrix was studied.
Silver and gold nano–particles where fabricated by firstly implanting 2×10^{16} ions/cm^2, 2 Mev ions in high quality fused silica substrates. Thereafter, the samples were annealed at 600 (Ag) and 1000 (Au) °C to obtain the nano–particles with known characteristics. During annealing, also most of the radiation defects are bleached so that the substrate is transparent at the laser's wavelength. In this case, we used a XeCl excimer laser with 55 ns FWHM width. Absorption occurs entirely at the nano–particles, by intraband transitions of the metal. However, as the heat conductivity is much larger for the metal, as the filling fraction of the metal is low (less than 2.5 %), and as the heat diffusion length (Eq. 9) for 55 ns is much larger than the mean separation distance between nano–particles, the temperature can be considered transversally homogenous and only a one dimensional heat transport problem considered. So, the source in Eq. 1 is due to the nano–particles. And as the nano–particles are not uniformly distributed as function of depth, the absorption coefficient α is considered to be a function of the depth and proportional to the amount of ions implanted. On the other hand, the conductivity and the heat capacity are governed by the matrix. The numerical solution of Eq. 1 shows that a minimum laser fluence (2 J/cm^2 in the Ag samples) is needed to take the system above the melting point of the metal. The maximum temperature in the sample occurs where the maximum density of nano–particles is found. The temperature profile for a 2.8 J/cm^2 pulse is shown in Fig. 6 (a). The maximum laser irradiance took place at $t_0 = 70$ ns. It can be observed that the temperature of the system is well above the melting point of silver. And this agrees well with the experimental results shown in Fig. 6 (b), where one can see that with laser fluences above 2 J/cm^2, the surface plasmon resonance broadens, indicating that the nano–particles become smaller. Increment of the thermal stress above the tensile strength occurs at the same time, and therefore, parts of the surface fall down leaving a square well behind, instead of the usual crater in normal surface ablation. The depth of the step matches the ion range.The same effect was observed with gold nano–particles, and could be explained in the same way.

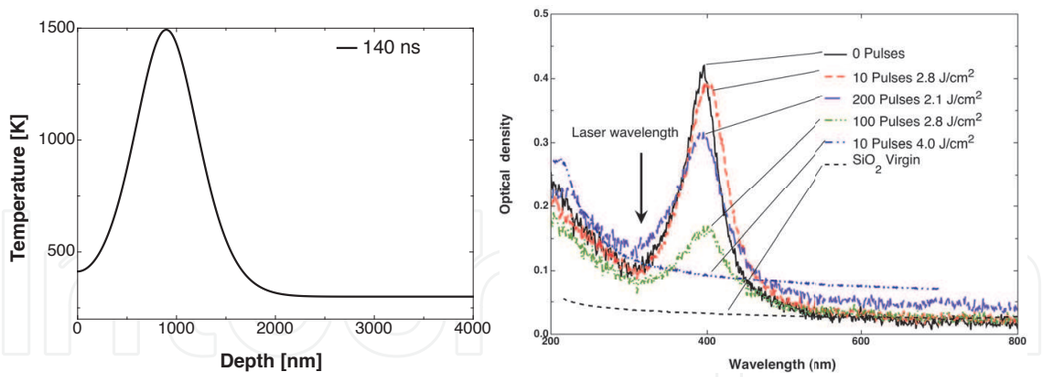

(a) Temperature profile. (b) Extinction spectra.

Fig. 6. Effects of excimer laser on silver nano–particles embedded in SiO_2: (a) Temperature profile as function of depth, 70 ns after the maximum irradiance of a 2.8 J/cm^2 pulse. (b) Extinction spectra of samples treated with increasing laser fluences.

By means of a 6 ns FWHM pulsed Nd:YAG laser at 1064 nm and at 532 nm (Crespo-Sosa & Schaaf (n.d.)), samples containing Ag and Au nano–particles, prepared with the same method described above, were also irradiated. At this wavelength, energy is absorbed mainly by the matrix and little or no reduction is observed in the nano–particles size as they do not melt. On the contrary, in Fig. 7, one can see, that the first 10 pulses remove the surface carbon deposited (few nanometers below the surface) during Ag and Au implantation, and therefore the "background" drops. After 100 pulses, the resonance has turned narrower, indicating a slight growth of the nano–particles, but this growth does not continue after 1000 or 10000 pulses. In this case, the calculation of the temperature evolution indicates no significant increment. This means that this slight growth is not produced by a thermal process, and that another mechanism must be present.

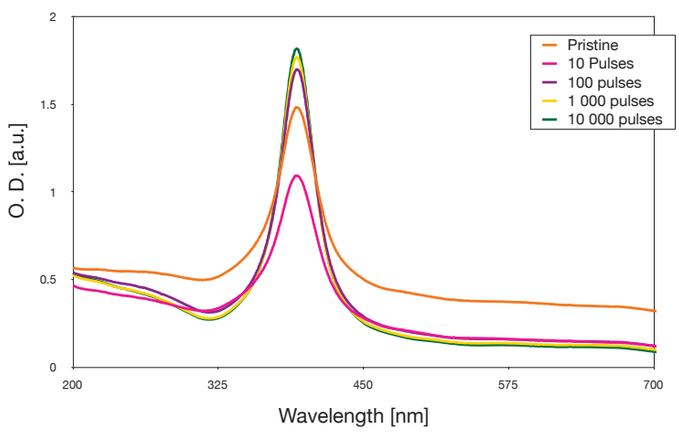

Fig. 7. Effects of infrared laser on Ag nano–particless embedded in SiO_2: Extinction spectra of samples treated with increasing number of pulses.

When irradiating these samples with a wavelength of 532 nm, we observed opposite effects between silver and gold nano–particles. This is because the resonance of gold nano–particles

falls very close to the irradiation wavelength, while the resonance for silver is around 400 nm. In other words, the system with Ag nano–particles absorbs the energy uniformly by the matrix, whereas Au nano–particles absorb the energy in the other case. By tunning the wavelength, one can select whether to provoke effects directly on the nano–particles or onto the matrix.

Nano–particles decomposition and accompanying surface ablation is usually related to the energy absorbed, the location and the duration of the pulse. The shorter the pulse is, the higher the temperature that the nano–particles can reach and therefore the lower the ablation threshold. This has been experimentally verified with nanosecond pulses, but with picosecond pulses, non thermal effects may appear. For example, when Ag nano–particles are irradiated with 26 ps pulses at 355 nm , a surprisingly high ablation threshold is found (Torres-Torres et al. (2010)). The cause for this, is not fully understood. The measured non-linear absorption coefficient is, from the thermal point of view, negligible to account for such an effect. On the other hand, it has been reported that two–photon absorption, (an equally improbable event) can be important in the determination of the melting threshold of silicon by ps laser pulses at 1064 nm (van Driel (1987)).

From a merely thermal point of view, the use of shorter laser pulses can be treated ”locally” as the heat diffusion length becomes shorter. Xia and co–workers have, for example, modeled the temperature evolution of a nano–particle embedded in a transparent matrix by means of Eq. 2. And from this calculation , they showed that the corresponding thermal stress and phase transformations are important in the description of surface ablation and of nano–particles fragmentation (Xia et al. (2006)). Picosecond and femtosecond pulses can provoke damage in materials that can also be treated thermally. It has been mentioned above, that typically, hot electrons transfer their energy to the lattice in times shorter than few picoseconds. When pulses shorter than this time are used, the dynamics of the electrons must be taken into account. Today’s main interest in such pulses is precisely the possibility of studying the dynamic evolution of the system. In this case, Eq. 2 is used to test if the fundamental parameters of the electron-electron and electron-phonon interactions are properly reproduced by the proposed model (Bertussi et al. (2005); Bruzzone & Malvaldi (2009); Dachraoui & Husinsky (2006); Muto et al. (2008); Zhang & Chen (2008)). It is in a certain way the inverse problem where the thermal properties are to be determined. Another fine example, where the calculation of the electronic temperature by means of Eq. 2 plays an important role, is the determination of the contribution of the hot electrons to the third–order non–linear susceptibility of gold nano–particles (Guillet et al. (2009)).

5. Discussion

As seen above, the methodology for studying the temperature increase in the material due to laser– or to ion–irradiation has been well established using the heat equation. However, let us make a few remarks on it:

Even though calculations are not too sensitive to changes in the values of the thermal properties, the uncertainty of them should always be a concern. The processes involved occur and also cause high pressure regions, where a state equation of the system can hardly be known. Additionally, the possibility of a change in these values in nano–structures must also be considered (Buffat & Borel (1976)). Also, the possibility of non–Fourier’s heat conduction has not been discussed enough (Cao & Guo (2007); Rashidi-Huyeh et al. (2008)). Indeed, it is not always clear how important a variation in such parameters is or how important the consideration of a particular effect is.

Another problem to be considered, is the cumulative nature of the effects. Most of the calculations are based on single events, an ion or a pulse, and then scaled, while events might be cumulative. Neither are charge effects considered in these kinds of calculation and they might, in some cases, have an important influence on the effects observed. Also, most of the calculations have been simplified to solve the one dimensional heat equation (Awazu et al. (2008)).

The process in which the ion deposits its energy to the nuclei of the target is highly stochastic. The ion does not follow a straight line and the energy deposition density (F_d) is not uniform. The process described by the heat equation, must be then considered as an "average" event, as in an statistical point of view. Furthermore, the description through the heat equation assumes thermal equilibrium and energy transfer, but during the first stages of the process, the energy is limited to only few atoms, that move with high kinetic energy, that might be better described by a ballistic approach. Indeed, there are effects (in ion beam mixing, for instance), that are directly related to the primary knock-on collisions, that cannot be described by the thermal equation.

The interaction of the ion with the electrons can be thought as more uniform because the electron density is much higher, but additional parameters arise, like the coupling function g in Eq. 2 and the thermal properties of the electronic cloud. In this case, the consideration of the "ballistic" range of the ejected electrons by the ion is important to input correctly the spatial deposition of energy.

Though in principle simpler, the interaction of high power lasers with matter also present interesting challenges to consider, first, the effects that raise due to high intensity pulses, in which the absorption and conductive processes might be altered within the same pulse, and the effects due to the ultrashort pulses that might be even faster than the system thermalization.

6. Conclusions

In this chapter, it has been reviewed how the simple, yet powerful concepts of classical heat conduction theory have been extended to phenomena like ion beam and laser effects on materials. These phenomena are characterized by the wide range of temperatures involved, extreme short times and high annealing and cooling rates, as well as by the nanometric spaces in which they occur. In consequence, there is a high uncertainty in the values of the thermal properties that must be used for the calculations. Nevertheless, the calculations done up-today have proved to be very useful to describe the effects of them. They also agree with other methods like Monte Carlo and molecular dynamics simulations. In the future these parameters must be better determined (theoretically and experimentally) and further applied to more complex systems, like nano–structured materials as well as to femto and atosecond processes. The knowledge of the fundamentals of radiation interaction behind these processes will benefit a lot from thess new experimental, theoretical and computational tools.

7. Aknowledgments

The author would like to thank all the colleagues, technicians and students that have participated in the experiments described above. And to the following funding organizations: CONACyT, DGAPA-UNAM, ICyTDF and DAAD.

8. References

Awazu, K., Wang, X., Fujimaki, M., Tominaga, J., Aiba, H., Ohki, Y. & Komatsubara, T. (2008). Elongation of gold nanoparticles in silica glass by irradiation with swift heavy ions, *Physical Review B* 78(5): 1–8.
URL: *http://link.aps.org/doi/10.1103/PhysRevB.78.054102*

Bertussi, B., Natoli, J., Commandre, M., Rullier, J., Bonneau, F., Combis, P. & Bouchut, P. (2005). Photothermal investigation of the laser-induced modification of a single gold nano-particle in a silica film, *Optics Communications* 254(4-6): 299–309.
URL: *http://linkinghub.elsevier.com/retrieve/pii/S0030401805005377*

Bruzzone, S. & Malvaldi, M. (2009). Local Field Effects on Laser-Induced Heating of Metal Nanoparticles, *The Journal of Physical Chemistry C* 113(36): 15805–15810.
URL: *http://pubs.acs.org/doi/abs/10.1021/jp9003517*

Buffat, P. & Borel, J. (1976). Size effect on melting temperature of gold particles, *Physical Review A* 13(6): 2287.
URL: *http://pra.aps.org/abstract/PRA/v13/i6/p2287_1*

Cao, B.-Y. & Guo, Z.-Y. (2007). Equation of motion of a phonon gas and non-Fourier heat conduction, *Journal of Applied Physics* 102(5): 053503.
URL: *http://link.aip.org/link/JAPIAU/v102/i5/p053503/s1&Agg=doi*

Cheang-Wong, J. C., Oliver, A., Crespo-Sosa, A., Hernández, J. M., Muñoz, E. & Espejel-Morales, R. (2000). Dependence of the optical properties on the ion implanted depth profiles in fused quartz after a sequential implantation with Si and Au ions, *Nuclear Instruments and Methods in Physics Research Section B: Beam Interactions with Materials and Atoms* 161-163: 1058–1063.
URL: *http://linkinghub.elsevier.com/retrieve/pii/S0168583X99009192*

Chettah, a., Kucal, H., Wang, Z., Kac, M., Meftah, a. & Toulemonde, M. (2009). Behavior of crystalline silicon under huge electronic excitations: A transient thermal spike description, *Nuclear Instruments and Methods in Physics Research Section B: Beam Interactions with Materials and Atoms* 267(16): 2719–2724.
URL: *http://linkinghub.elsevier.com/retrieve/pii/S0168583X09006569*

Crespo-Sosa, A. & Schaaf, P. (n.d.). Unpublished.

Crespo-Sosa, A., Schaaf, P., Reyes-Esqueda, J. A., Seman-Harutinian, J. A. & Oliver, A. (2007). Excimer laser absorption by metallic nano-particles embedded in silica, *Journal of Physics D: Applied Physics* 40(7): 1890–1895.
URL: *http://stacks.iop.org/0022-3727/40/i=7/a=008?key=crossref.f57509912f821b768966f484bf900042*

Dachraoui, H. & Husinsky, W. (2006). Fast electronic and thermal processes in femtosecond laser ablation of Au, *Applied Physics Letters* 89(10): 104102.
URL: *http://link.aip.org/link/APPLAB/v89/i10/p104102/s1&Agg=doi*

Daraszewicz, S. & Duffy, D. (2010). Extending the inelastic thermal spike model for semiconductors and insulators, *Nuclear Instruments and Methods in Physics Research Section B: Beam Interactions with Materials and Atoms* 269(14): 1646–1649.
URL: *http://linkinghub.elsevier.com/retrieve/pii/S0168583X10008566*

D'Orléans, C., Stoquert, J., Estournès, C., Cerruti, C., Grob, J., Guille, J., Haas, F., Muller, D. & Richard-Plouet, M. (2003). Anisotropy of Co nanoparticles induced by swift heavy ions, *Physical Review B* 67(22): 10–13.
URL: *http://link.aps.org/doi/10.1103/PhysRevB.67.220101*

D'Orléans, C., Stoquert, J., Estournes, C., Grob, J., Muller, D., Cerruti, C. & Haas, F. (2004). Deformation yield of Co nanoparticles in SiO_2 irradiated with 200 MeV ^{127}I ions, *Nuclear Instruments and Methods in Physics Research Section B: Beam Interactions with Materials and Atoms* 225(1-2): 154–159.
URL: *http://linkinghub.elsevier.com/retrieve/pii/S0168583X04007852*

D'Orléans, C., Stoquert, J., Estournes, C., Grob, J., Muller, D., Guille, J., Richardplouet, M., Cerruti, C. & Haas, F. (2004). Elongated Co nanoparticles induced by swift heavy ion irradiations, *Nuclear Instruments and Methods in Physics Research Section B: Beam Interactions with Materials and Atoms* 216(1-2): 372–378.
URL: *http://linkinghub.elsevier.com/retrieve/pii/S0168583X03021736*

Duffy, D. M., Itoh, N., Rutherford, a. M. & Stoneham, a. M. (2008). Making tracks in metals, *Journal of Physics: Condensed Matter* 20(8): 082201.
URL: *http://stacks.iop.org/0953-8984/20/i=8/a=082201?key=crossref.47f54125ceffe4f9f25b4fd4082dde60*

Duffy, D. M. & Rutherford, a. M. (2007). Including the effects of electronic stopping and electron-ion interactions in radiation damage simulations, *Journal of Physics: Condensed Matter* 19(1): 016207.
URL: *http://stacks.iop.org/0953-8984/19/i=1/a=016207?key=crossref.cc3ab92c89a9b411156b1a3956294e00*

Elsayed-Ali, H., Norris, T., Pessot, M. & Mourou, G. (1987). Time-Resolved Observation of Electron-Phonon Relaxation in Copper, *Physical Review Letters* 58(12): 1212–1215.
URL: *http://link.aps.org/doi/10.1103/PhysRevLett.58.1212*

Giulian, R., Kluth, P., Araujo, L., Sprouster, D., Byrne, A., Cookson, D. & Ridgway, M. (2008). Shape transformation of Pt nanoparticles induced by swift heavy-ion irradiation, *Physical Review B* 78(12): 1–8.
URL: *http://link.aps.org/doi/10.1103/PhysRevB.78.125413*

Johannessen, B., Kluth, P., Giulian, R., Araujo, L., Leewelin, D.J., Foran, G.J., Cookson, D. & Ridgway, M. (2008). Modification of embedded Cu Nano–particles: Ion irradiation at room temperature., *Nuclear Instruments and Methods in Physics Research Section B: Beam Interactions with Materials and Atoms* 257(1-2): 37–41.
URL:

Guillet, Y., Rashidi–Huyeh, M. & Palpant. B. (2009). Influence of laser Pulse characteristics on the hot electron contribution to the third–order nonlinear optical response of gold nanoparticles., *Physical Review B* 79: 045410.
URL:

Katz, R. & Varma, M. N. (1991). Radial distribution of dose., *Basic life sciences* 58: 163–79; discussion 179–80.
URL: *http://www.ncbi.nlm.nih.gov/pubmed/1811472*

Klaumunzer, S. (2006). Modification of nanostructures by high-energy ion beams, *Nuclear Instruments and Methods in Physics Research Section B: Beam Interactions with Materials and Atoms* 244(1): 1–7.
URL: *http://linkinghub.elsevier.com/retrieve/pii/S0168583X05019002*

Kluth, P., Giulian, R., Sprouster, D. J., Schnohr, C. S., Byrne, a. P., Cookson, D. J. & Ridgway, M. C. (2009). Energy dependent saturation width of swift heavy ion shaped embedded Au nanoparticles, *Applied Physics Letters* 94(11): 113107.
URL: *http://link.aip.org/link/APPLAB/v94/i11/p113107/s1&Agg=doi*

Kluth, P., Johannessen, B., Giulian, R., Schnohr, C. S., Foran, G. J., Cookson, D. J., Byrne, A. P. & Ridgway, M. C. (2007). Ion irradiation effects on metallic nanocrystals, *Radiation Effects and Defects in Solids* 162(7): 501–513.
URL: *http://www.informaworld.com/openurl?genre=article&doi=10.1080/10420150701472221&magic=crossref||D404A21C5BB053405B1A640AFFD44AE3*

Lin, Z. & Zhigilei, L. (2007). Temperature dependences of the electron-phonon coupling, electron heat capacity and thermal conductivity in Ni under femtosecond laser irradiation, *Applied Surface Science* 253(15): 6295–6300.
URL: *http://linkinghub.elsevier.com/retrieve/pii/S0169433207000815*

Meldrum, A., Boatner, L. & White, C. (2001). Nanocomposites formed by ion implantation: Recent developments and future opportunities, *Nuclear Instruments and Methods in Physics Research Section B: Beam Interactions with Materials and Atoms* 178(1-4): 7–16.
URL: *http://linkinghub.elsevier.com/retrieve/pii/S0168583X00005012*

Mota-Santiago, P. E., Crespo-Sosa, A., Jiméenez-Hernáandez, J. L., Silva-Pereyra, H.-G., Reyes-Esqueda, J. A. & Oliver, A. (2011). Noble-Metal Nano-Crystal Aggregation in Sapphire by Ion Irradiation And Subsequent Thermal Annealing, *Journal of Physics D: Applied Physics* submitted.

Mota-Santiago, P. E., Crespo-Sosa, A., Jiméenez-Hernáandez, J. L., Silva-Pereyra, H.-G., Reyes-Esqueda, J. A. & Oliver, A. (2012). Ion beam induced deformation of gold nano-particles embedded in Sapphire.

Muto, H., Miyajima, K. & Mafune, F. (2008). Mechanism of Laser-Induced Size Reduction of Gold Nanoparticles As Studied by Single and Double Laser Pulse Excitation, *Journal of Physical Chemistry C* 112(15): 5810–5815.
URL: *http://pubs.acs.org/cgi-bin/doilookup/?10.1021/jp711353m*

Oliver, A., Reyes-Esqueda, J. A., Cheang-Wong, J. C., Román-Velázquez, C., Crespo-Sosa, A., Rodríguez-Fernández, L., Seman-Harutinian, J. A. & Noguez, C. (2006). Controlled anisotropic deformation of Ag nanoparticles by Si ion irradiation, *Physical Review B* 74(24): 1–6.
URL: *http://link.aps.org/doi/10.1103/PhysRevB.74.245425*

Penninkhof, J. J., Polman, A., Sweatlock, L. a., Maier, S. a., Atwater, H. a., Vredenberg, a. M. & Kooi, B. J. (2003). Mega-electron-volt ion beam induced anisotropic plasmon resonance of silver nanocrystals in glass, *Applied Physics Letters* 83(20): 4137.
URL: *http://link.aip.org/link/APPLAB/v83/i20/p4137/s1&Agg=doi*

Penninkhof, J. J., van Dillen, T., Roorda, S., Graf, C., Vanblaaderen, A., Vredenberg, a. M. & Polman, A. (2006). Anisotropic deformation of metallo-dielectric core-shell colloids under MeV ion irradiation, *Nuclear Instruments and Methods in Physics Research Section B: Beam Interactions with Materials and Atoms* 242(1-2): 523–529.
URL: *http://linkinghub.elsevier.com/retrieve/pii/S0168583X05015922*

Rangel-Rojo, R., Reyes-Esqueda, J. A., Torres-Torres, C., Oliver, A., Rodríguez-Fernández, L., Crespo-Sosa, A., Cheang-Wong, J. C., McCarthy, J., Bookey, H. & Kar, A. (2010). Linear and nonlinear optical properties of aligned elongated silver nanoparticles embedded in silica, *in* D. Pozo Perez (ed.), *Silver Nanoparticles*, InTech, pp. 35 – 62.
URL: *http://www.intechopen.com/articles/show/title/linear-and-nonlinear-optical-properties-of-aligned-elongated-silver-nanoparticles-embedded-in-silica*

Rashidi-Huyeh, M., Volz, S. & Palpant, B. (2008). Non-Fourier heat transport in metal-dielectric core-shell nanoparticles under ultrafast laser pulse excitation,

Physical Review B 78(12): 1–8.
URL: *http://link.aps.org/doi/10.1103/PhysRevB.78.125408*

Ridgway, M., Giulian, R., Sprouster, D., Kluth, P., Araujo, L., Llewellyn, D., Byrne, a., Kremer, F., Fichtner, P., Rizza, G., Amekura, H. & Toulemonde, M. (2011). Role of Thermodynamics in the Shape Transformation of Embedded Metal Nanoparticles Induced by Swift Heavy-Ion Irradiation, *Physical Review Letters* 106(9): 1–4.
URL: *http://link.aps.org/doi/10.1103/PhysRevLett.106.095505*

Rodríguez-Iglesias, V., Peña Rodríguez, O., Silva-Pereyra, H.-G., Rodríguez-Fernández, L., Cheang-Wong, J. C., Crespo-Sosa, A., Reyes-Esqueda, J. A. & Oliver, A. (2010). Tuning the aspect ratio of silver nanospheroids embedded in silica., *Optics letters* 35(5): 703–5.
URL: *http://www.ncbi.nlm.nih.gov/pubmed/20195325*

Ryazanov, A., Volkov, A. & Klaumünzer, S. (1995). Model of track formation, *Physical Review B* 51(18): 12107–12115.
URL: *http://link.aps.org/doi/10.1103/PhysRevB.51.12107*

Sands, D. (2011). Pulsed laser heating and melting, *in* Vyacheslav S. Vikhrenko (ed.), *Heat Conduction / Book 2*, InTech, pp. .
URL: *http://www.intechopen.com/*

Schmidt, B., Heinig, K.-H., Mücklich, A. & Akhmadaliev, C. (2009). Swift-heavy-ion-induced shaping of spherical Ge nanoparticles into disks and rods, *Nuclear Instruments and Methods in Physics Research Section B: Beam Interactions with Materials and Atoms* 267(8-9): 1345–1348.
URL: *http://linkinghub.elsevier.com/retrieve/pii/S0168583X09000834*

Schoenlein, R., Lin, W., Fujimoto, J. & Eesley, G. (1987). Femtosecond Studies of Nonequilibrium Electronic Processes in Metals, *Physical Review Letters* 58(16): 1680–1683.
URL: *http://link.aps.org/doi/10.1103/PhysRevLett.58.1680*

Silva-Pereyra, H.-G. (2011). *Estudio de los mecanismos de deformacióon de nano-partíiculas de oro embebidas en síilice, producidas por implantacióon de iones.*, PhD thesis, Universidad Nacional Autóonoma de Méexico.

Silva-Pereyra, H.-G., Arenas-Alatorre, J., Rodríguez-Fernández, L., Crespo-Sosa, A., Cheang-Wong, J. C., Reyes-Esqueda, J. A. & Oliver, A. (2010). High stability of the crystalline configuration of Au nanoparticles embedded in silica under ion and electron irradiation, *Journal of Nanoparticle Research* 12(5): 1787–1795.
URL: *http://www.springerlink.com/index/10.1007/s11051-009-9735-6*

Sun, C., Vallée, F., Acioli, L., Ippen, E. & Fujimoto, J. (1994). Femtosecond-tunable measurement of electron thermalization in gold., *Physical review. B, Condensed matter* 50(20): 15337–15348.
URL: *http://www.ncbi.nlm.nih.gov/pubmed/9975886*

Takeda, Y. & Kishimoto, N. (2003). Nonlinear optical properties of metal nanoparticle composites for optical applications, *Nuclear Instruments and Methods in Physics Research Section B: Beam Interactions with Materials and Atoms* 206: 620–623.
URL: *http://linkinghub.elsevier.com/retrieve/pii/S0168583X03007973*

Torres-Torres, C., Peréa-López, N., Reyes-Esqueda, J. A., Rodríguez-Fernández, L., Crespo-Sosa, A., Cheang-Wong, J. C. & Oliver, A. (2010). Ablation and optical third-order nonlinearities in Ag nanoparticles., *International journal of nanomedicine* 5: 925–32.

URL: *http://www.pubmedcentral.nih.gov/articlerender.fcgi?artid=3010154&tool=pmcentrez&rendertype=abstract*

Toulemonde, M. (2000). Transient thermal processes in heavy ion irradiation of crystalline inorganic insulators, *Nuclear Instruments and Methods in Physics Research Section B: Beam Interactions with Materials and Atoms* 166-167: 903–912.
URL: *http://linkinghub.elsevier.com/retrieve/pii/S0168583X99007995*

Toulemonde, M., Assmann, W., Trautmann, C., Gruner, F., Mieskes, H., Kucal, H. & Wang, Z. (2003). Electronic sputtering of metals and insulators by swift heavy ions, *Nuclear Instruments and Methods in Physics Research Section B: Beam Interactions with Materials and Atoms* 212: 346–357.
URL: *http://linkinghub.elsevier.com/retrieve/pii/S0168583X0301721X*

Toulemonde, M., Dufour, C. & Paumier, E. (1992). Transient thermal process after a high-energy heavy-ion irradiation of amorphous metals and semiconductors, *Physical Review B* 46(22): 14362–14369.
URL: *http://link.aps.org/doi/10.1103/PhysRevB.46.14362*

Toulemonde, M., Trautmann, C., Balanzat, E., Hjort, K. & Weidinger, a. (2004). Track formation and fabrication of nanostructures with MeV-ion beams, *Nuclear Instruments and Methods in Physics Research Section B: Beam Interactions with Materials and Atoms* 216: 1–8.
URL: *http://linkinghub.elsevier.com/retrieve/pii/S0168583X03021025*

Trinkaus, H. (1998). dynamics of viscoelastic flow in ion tracks: origin of platic deformation of amorphous materials, *Nuclear Instruments and Methods in Physics Research B* 146: 204–216.

van Dillen, T., Polman, A., Onck, P. & van der Giessen, E. (2005). Anisotropic plastic deformation by viscous flow in ion tracks, *Physical Review B* 71(2): 1–12.
URL: *http://link.aps.org/doi/10.1103/PhysRevB.71.024103*

van Driel, H. (1987). Kinetics of high-density plasmas generated in Si by 1.06- and 0.53-μm picosecond laser pulses, *Physical Review B* 35(15): 8166–8176.
URL: *http://prb.aps.org/abstract/PRB/v35/i15/p8166_1 http://link.aps.org/doi/10.1103/PhysRevB.35.8166*

Vineyard, G. H. (1976). Thermal spikes and activated processes, *Radiation Effects and Defects in Solids* 29(4): 245–248.
URL: *http://www.informaworld.com/openurl?genre=article&doi=10.1080/00337577608233050&magic=crossref||D404A21C5BB053405B1A640AFFD44AE3*

Waligórski, M. P. R., Hamm, R. N. & Katz, R. (1986). The Radial Distribution of Dose around the Path of a Heavy Ion in Liquid Water, *Nuclear Tracks and Radiation Measurements* 11(6): 309–319.

Wang, Z., Dufour, C., Paumier, E. & Toulemonde, M. (1994). The Se sensitivity of metals under swift-heavy-ion irradiation: a transient thermal process, *Journal of Physics: Condensed Matter* 6: 6733.
URL: *http://iopscience.iop.org/0953-8984/6/34/006*

Xia, Z., Shao, J., Fan, Z. & Wu, S. (2006). Thermodynamic damage mechanism of transparent films caused by a low-power laser., *Applied optics* 45(32): 8253–61.
URL: *http://www.ncbi.nlm.nih.gov/pubmed/17068568*

Zhang, Y. & Chen, J. K. (2008). Ultrafast melting and resolidification of gold particle irradiated by pico- to femtosecond lasers, *Journal of Applied Physics* 104(5): 054910.
URL: *http://link.aip.org/link/JAPIAU/v104/i5/p054910/s1&Agg=doi*

Heat Transfer - Engineering Applications
Edited by Prof. Vyacheslav Vikhrenko

ISBN 978-953-307-361-3
Hard cover, 400 pages
Publisher InTech
Published online 22, December, 2011
Published in print edition December, 2011

Heat transfer is involved in numerous industrial technologies. This interdisciplinary book comprises 16 chapters dealing with combined action of heat transfer and concomitant processes. Five chapters of its first section discuss heat effects due to laser, ion and plasma-solid interaction. In eight chapters of the second section engineering applications of heat conduction equations to the curing reaction kinetics in manufacturing process, their combination with mass transport or ohmic and dielectric losses, heat conduction in metallic porous media and power cables are considered. Analysis of the safety of mine hoist under influence of heat produced by mechanical friction, heat transfer in boilers and internal combustion engine chambers, management for ultrahigh strength steel manufacturing are described in this section as well. Three chapters of the last third section are devoted to air cooling of electronic devices.

InTech Europe
University Campus STeP Ri
Slavka Krautzeka 83/A
51000 Rijeka, Croatia
Phone: +385 (51) 770 447
Fax: +385 (51) 686 166
www.intechopen.com

InTech China
Unit 405, Office Block, Hotel Equatorial Shanghai
No.65, Yan An Road (West), Shanghai, 200040, China
中国上海市延安西路65号上海国际贵都大饭店办公楼405单元
Phone: +86-21-62489820
Fax: +86-21-62489821

IntechOpen